processes

MDPI

Article

Experimental Study on Fractal Characteristics of Adsorption Pore Structure of Coal

Wendi Wang [1,2], Zhen Liu [1,2,*], Mingrui Zhang [1,2] and He Yang [1,2]

[1] College of Safety and Environmental Engineering, Shandong University of Science and Technology, 579 Qianwangang Rd., Huangdao District, Qingdao 266590, China
[2] State Key Laboratory of Mining Disaster Prevention and Control Co-Founded by Shandong Province and the Ministry of Science and Technology, Shandong University of Science and Technology, Qingdao 266590, China
* Correspondence: liuzhensdust@sdust.edu.cn; Tel.: +86-13954252676

Abstract: The adsorption pore structure is the key affecting the technology of enhanced coal bed methane recovery (ECBM). In this paper, nitrogen adsorption measurement (NAM) and low-field nuclear magnetic resonance (NMR) methods are used to test the structural parameters of adsorption pores of four coal samples with different metamorphic degrees. Combining with the fractal theory, the applicability and the physical significance of fractal dimensions obtained from different models are analyzed. Finally, the main factors affecting the complexity of the pore size structure and the influence of fractal characteristics on the adsorption properties of coal are discussed. The results show that with the increase in the degree of metamorphism, the ranking order of the volume and the specific surface area of adsorption pores of four coal samples are long flame coal > anthracite > gas coal > coking coal. The fractal dimension D_2 calculated by the Frenkel–Halsey–Hill (FHH) fractal model ranges from 2.5 to 2.9, representing the degree of the pore surface irregularity, and D_3 calculated by the FHH fractal model ranges from 2.004 to 2.037, representing the complexity of pore size distribution. There is no clear quantitative relationship between the fractal dimension and the single structure parameters of adsorption pores. The more the pore diameter distribution is concentrated in the range of 2–5 nm, the larger the fractal dimension is, the higher the complexity of adsorption pore structure is; D_2, which represents the irregularity of the surface of coal, has a good linear positive correlation with the maximum adsorption capacity of N_2.

Keywords: fractal dimension; pore structure; pores characteristics; fractal theory; metamorphism

Citation: Wang, W.; Liu, Z.; Zhang, M.; Yang, H. Experimental Study on Fractal Characteristics of Adsorption Pore Structure of Coal. *Processes* **2023**, *11*, 78. https://doi.org/10.3390/pr11010078

Academic Editors: Feng Du, Aitao Zhou and Bo Li

Received: 2 December 2022
Revised: 24 December 2022
Accepted: 25 December 2022
Published: 28 December 2022

1. Introduction

As an extremely important unconventional natural gas energy, coal bed methane (CBM) resources have attracted great attention from the energy community around the world [1–6]. Unlike conventional natural gas reservoirs, the nano-scale adsorption pore structure of coal is the important storage space for gas. And its structural characteristics directly determine the gas adsorption and desorption process, thereby affecting the gas content of coal seams [7,8]. Therefore, studying the characteristics of the coal adsorption pore structure is the basis for revealing the law of the coalbed methane adsorption–desorption–diffusion migration [9,10]. At present, scholars have mainly researched the coal structure based on image analyses, fluid injection, and gas adsorption methods [11–13]. For example, Feng et al. [14] used scanning electron microscopy (SEM) and computer tomography (CT) to analyze the microstructure and deformation of coal samples after the methane adsorption process; Meng and Qiu [15] studied the mechanism of the spatial diffusion of coal samples after supercritical CO_2 treatment through SEM, mercury intrusion porosimetry (MIP), and nuclear magnetic resonance (NMR). Simultaneously, due to the wide distribution of coalbed methane reservoirs in China

and the variety of coal, the degree metamorphism of coal can affect its internal reservoir space. Scholars have also carried out extensive research on this [16]. There are several examples. Chen et al. [17] used the Fourier transform infrared (FTIR) spectrometer and CO_2 adsorption methods to study the micropore characteristics of five coal samples with different metamorphism degrees; Niu et al. [18] used the liquid nitrogen method and the methane isotherm adsorption experiment to study the pore structure and adsorption properties of 12 different rank coals. Therefore, based on previous studies, this paper uses the classic experimental methods to carry out multi-scale structural analyses of coal with different degrees of metamorphism to accurately and quantitatively characterize the structural characteristics of coal at the adsorption pore scale.

Coal is a porous medium with a complex structure and the experimental study of its heterogeneity is a key to the microstructure of coal [19,20]. At present, the fractal theory represents the effectiveness of the space occupied by complex shapes. It is a measure of the irregularity of complex shapes that can be introduced instead of characterizing the "special nature" of the coal pore structure [21–23]. Through the research of domestic and foreign scholars, the models for calculating the fractal size of pore structure include FHH model, Menger sponge model, and other applicability models [22,24,25]. In several proposed fractal models, the FHH fractal model is used to discuss the extent to which the internal surface roughness of coal determines the amount of natural gas, especially methane. They can readily adsorb/store, and the gas can easily flow and be produced from coal formations. Cai et al. [26] studied the physical composition and particle size distribution of coal by integrating classical geometric fractal model and thermodynamic fractal model. Lu et al. [27] explored the fitting of Sierpinski, Menger, and other models to coal pore structure at different scales, and summarized the fractal characteristics of coal adsorption pore structure. Hu et al. [28] combined fractal model and image analysis to explore the fractal dimension of coke particles and describe the surface characteristics of coal and coke particles. Liu et al. [29] calculated the adsorption pore volume based on the capillary bubble fractal model and NMR T_2 spectrum distribution, thus quantitatively characterizing the physical structure of coal. Scholars have quantitatively characterized the fractal characteristics of coal structures in detail, but have not made a detailed mechanistic explanation for the type of coal structures complexity represented by the fractal model. This paper has carried out certain research based on this.

According to previous studies, scholars have carried out detailed quantitative characterization of the fractal characteristics of coal structure, but there is little research on the type of coal structure complexity represented by the fractal model. On this basis, this paper has carried out some research. The selection of appropriate experimental methods and fractal models, accurate and quantitative analysis of the change law of coal structural parameters with different degrees of metamorphism to clarify the influence mechanism of coal microstructure parameters on fractal characteristics, as well as the detailed physical significance and important influencing factors of fractal models, are the key research contents of this paper. In this paper, NAM and NMR are selected to analyze the multi-scale structural characteristics of adsorption pores ($r < 50$ nm) [30] of coal with different metamorphism degrees according to the metamorphic characteristics of four coal samples. At the same time, the difference and applicability of the fractal dimension of adsorption pore structure combined with FHH model and capillary bundle model are comprehensively analyzed. Finally, the relationships between structural parameters and fractal dimensions are discussed, and based on this, the important factors affecting the pore structure complexity are clarified. The above research is the key to reveal the influence mechanism between the geological evolution process of the coalbed methane reservoir and the distribution law of gas content. It is of great significance for mine gas disaster prevention and coalbed methane research.

2. Materials and Experiments

2.1. Samples

This laboratory experiment selects raw coal from four coal mines in Shaanxi, Shandong, Anhui, and Shanxi provinces of China. Bulk raw coal samples obtained on site are transported to the laboratory for the industrial analyses, Table 1 shows the analysis results. And raw coals are used in both experiments. Four lump coal samples with a mass slightly greater than 0.1 g were used in NAM experiment, with a total area of 2–50 m^2/g. In the NMR experiment, four kinds of lump coal samples are made into experimental coal samples with a diameter of 25 mm and a height of 50 mm by using equipment.

Table 1. The industrial analyses/%.

Number	Samples	M_{ad}	A_{ad}	V_{da}	FC_{daf}	Vitrinite	Inertinite	Exinite	Ro_{max}
1	DLT	6.29	9.7	28.98	55.03	87.01	11.89	1.10	0.53
2	XLZ	3.08	5.21	30.06	61.65	64.37	23.82	11.81	0.78
3	QD	1.38	23.61	19.53	55.48	63.82	34.72	1.46	1.38
4	QC	1.83	17.35	15.84	64.98	55.51	43.67	0.82	1.87

Note: No. 1 is long flame coal; No. 2 is gas coal; No. 3 is coking coal; and No. 4 is anthracite. The metamorphic degree ranking order of the four kinds of coal samples is #1−DLT < #2−XLZ < #3−QD < #4−QC. M_{ad} is the moisture; A_d is the content ash; V_{da} is the volatile matter; FC_{daf} is the fixed carbon; Ro_{max} is the maximum reflectance of vitrinite.

2.2. NAM and NMR

For the NAM analyses, the four kinds of coal samples are tested with a Micromeritics ASAP2020 BET specific surface area and pore diameter analyzer. The samples are heated, dehydrated and degassed, cooled, and weighed in turn. Then, the samples are put into the instrument for measurement and analyses, and the adsorption and desorption isotherms of coal samples are obtained. Finally, the pore structure parameters of coal samples are obtained through the BET, BJH, and DFT models. For the NMR analyses, four kinds of coal samples are tested with the MesoMR23-060H low-field NMR equipment. The magnet of the instrument is a permanent magnet, the magnetic field strength is 0.5 T, the main frequency is 11 MHz, the diameter of the probe coil is 60 mm, the echo time (TE) is 0.1 ms, the number of echoes is 6000, the number of scanning is 64, and the experimental environment temperature is 25.5 °C. First, the coal samples are dried at 60 °C to remove the impurities; second, the samples are vacuumized, and the coal samples are placed in water for 48 h for the saturated water treatment. The coal sample before the NMR experiment does not have additional pressure on it during the 48-h saturated water treatment process, and because the water is an incompressible fluid, it will not destroy the pore structure of the original coal sample, so it will not affect the NMR experimental results. Finally, the samples are taken out to test the saturated water samples, and the T_2 relaxation distributions are calculated by using the simultaneous iterative reconstruction technique, and the number of iterations is 10,000. Because the NMR is based on the spin motion of the hydrogen nucleus, the amplitude of the T_2 spectrum of coal samples measured in this experiment can reflect the total hydrogen content of a certain pore diameter. Three different relaxation mechanisms affecting T_2 spectrum are: the free relaxation, the surface relaxation, and the diffusion relaxation. When the three relaxation mechanisms exist simultaneously, the T_2 of the fluid in the pore can be expressed as [31]:

$$\frac{1}{T_2} = \frac{1}{T_{2B}} + \frac{1}{T_{2S}} + \frac{1}{T_{2D}} \quad (1)$$

In Equation (1), T_{2B} is the free relaxation time; T_{2S} is the surface relaxation time; T_{2D} is the diffusion relaxation time.

The experiment is that pure fluid (water) is carried out under the uniform magnetic field, so the effect of diffusion and free relaxation is not considered. Then only the surface relaxation is considered. The surface relaxation is from the relaxation action of coal particle

surface to fluid, which is related to the ratio of specific surface area to pore volume in the coal sample. Then Equation (1) can be simplified as follows:

$$\frac{1}{T_2} = \frac{1}{T_{2S}} = \rho_2 \left(\frac{S}{V}\right)_{pore} \tag{2}$$

In Equation (2), T_2 is the relaxation time; ρ_2 is the surface relaxation rate of T_2; it can be directly related to capillary force and pore diameter, S is the pore surface area; V is the pore volume; $\left(\frac{S}{V}\right)_{\text{porosity}}$ is the specific surface area of pores, the relationship between the pore radius and pore size is $\left(\frac{S}{V}\right)_{pore} = \frac{F_s}{r}$; F_s is the shape factor, which is determined by the pore model. Therefore, Equation (3) can be expressed as [32]:

$$T_2 = \frac{1}{\rho_2 F_s} r \tag{3}$$

Let $\frac{1}{\rho_2 F_s} = C$, then the Equation (3) can be expressed as $T_2 = C \times r$, and the coefficient C is the constant. After the value of C is obtained, the NMR T_2 spectrum can be converted into the pore radius distribution. Therefore, the pore size distribution of coal samples can be obtained according to the T_2 spectrum distribution. Figure 1 is the experimental equipment and experimental schematic diagram.

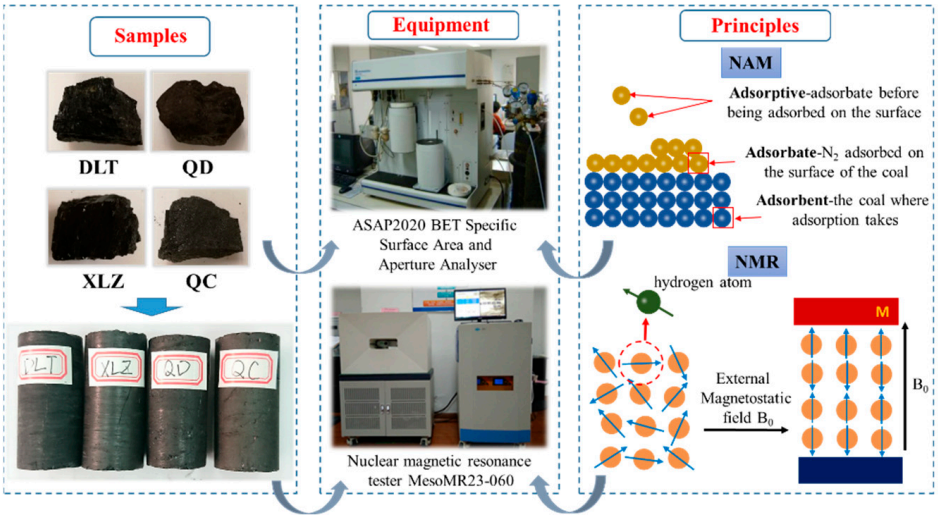

Figure 1. Experimental equipment and principles.

3. Results

3.1. Experimental Results of NAM

Through the NAM, the adsorption and desorption curves of coal samples are obtained, as shown in Figure 2. From Figure 2, the adsorption and desorption curves of four coal samples all present the inverted "S" type shape, which is the type II adsorption isotherm. When the adsorption capacity of the desorption branch is greater than that of the adsorption branch at the same relative pressure, the adsorption branch and the desorption branch do not coincide in a certain range of the relative pressure, and the separated loop is called the "hysteresis loop" [33]. Hysteresis loop can be divided into two types according to its shape, the first type of curve is shown in Figure 2a, and the second type of curve is shown in Figure 2b–d. Classification by BDDT and IUPAC [34], the shape of the first kind of hysteresis loop is basically consistent with the H2 (b) curve type, which indicates that it is characterized by the large adsorption loop, obvious hysteresis loop, and inflection point. It is further indicated that the adsorption pore system of low-rank coal is more complex, and there are "ink bottle" pores with small mouths and large bellies. The shape of the second kind of the hysteresis loop is basically consistent with that of H3 type, which indicates that the adsorption loop is small,

the hysteresis loop is not obvious, and there is a slight inflection point. Then it shows that the adsorption pore system of medium and high rank coal is relatively simple, and flat slit capillary pores are present. Among them, the size of the second type of hysteresis loop shows the following trend: #2−XLZ < #3−QD < #4−QC, and it can be concluded that it increases with the increase in coal metamorphism degree [35].

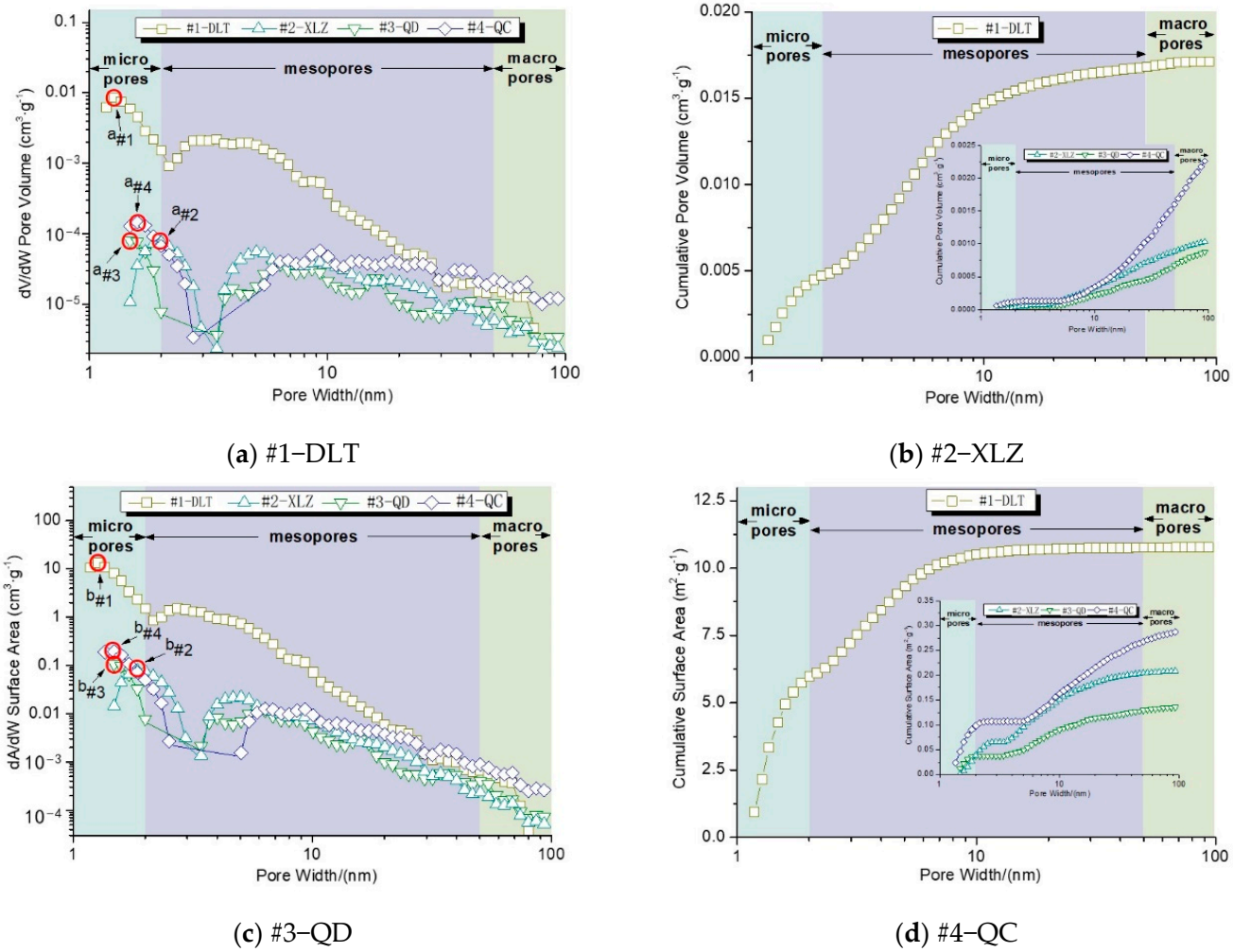

(**a**) #1−DLT (**b**) #2−XLZ

(**c**) #3−QD (**d**) #4−QC

Figure 2. Adsorption and desorption curves of the four coal samples.

The data analysis module of the adsorption instrument used in the experiment includes many classical model algorithms (such as BET, BJH, H-K, t-plot and NLDFT models).

On this basis, the nonlocal density function theory (NLDFT), which is an effective method to describe the fluid behavior in pores at the molecular level, is selected. It is assumed that the adsorption isotherms are obtained by multiplying numerous individual "single pore" adsorption isotherms by the relative distribution f(W) of their coverage pore size range. As long as the adsorbent and absorbent are given in the system, a set of influence functions (kernels) can be obtained by DFT simulation, and then the pore size distribution curve is obtained by solving the equation by fast non-negative least squares method. The pore size distribution characterized by it can be applied to the entire range of adsorption pores in coal samples [36]. Four pore size distributions (DV/DW, cumulative pore volume, DA/DW, and cumulative specific surface area) are plotted, as shown in Figure 3.

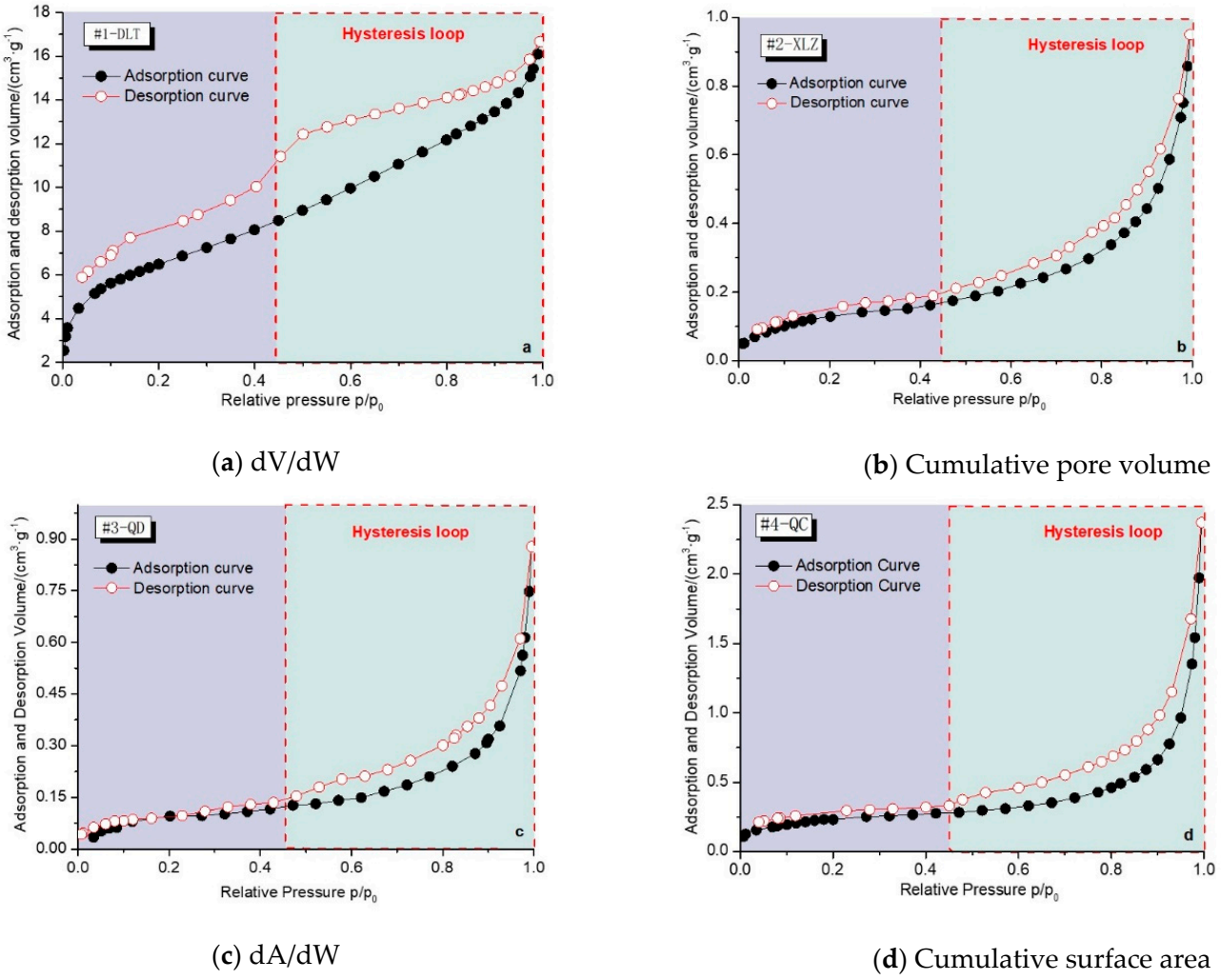

Figure 3. The pore size distribution measured with the NAM.

The IUPAC pore classification standard [37] is adopted in this test. The adsorption pore range of coal samples tested includes micropore (<2 nm), mesopore (2 nm $\leq D \leq$ 50 nm), and macropore (50 nm < D < 90 nm). According to Figure 3, the pore size distribution curves of four coal samples are within the microporous scale range, showing the single peak characteristic, with the highest peak point, but the peak values are different, that is, a#1 > a#4 > a#2 ≈ a#3 and b#1 > b#4 > b#2 ≈ b#3. That is to say, within this range, the pore volume and specific surface area decrease first and then increase with the increase of the metamorphic degree, and the micropore volume and surface area of #1−DLT coal sample with the lowest metamorphic degree among four coal samples are the largest. In the range of mesoporous scale, only the #1−DLT coal sample shows the single peak characteristic, and the highest peak point is close to the pore scale boundary of 2 nm. The other three coal samples show complex multi peak characteristics, which are mostly concentrated at 10 nm–50 nm. However, the average peak sizes of four coal samples are different, #1−DLT > #4−QC > #2−XLZ > #3−QD, which indicates that the #1−DLT coal sample has the largest mesoporous pore volume and specific surface area. In the whole range of mesoporous scale, the distribution of mesoporous concentration of the #1−DLT coal sample is close to the boundary of the micro-meso porous scale range, while the distribution trend of the other three coal samples is close to the boundary of the macropore scale range. In the macropore pore scale, due to the limitation of the gas adsorption method, the variation characteristics are not obvious, and the volume and specific surface area change little with the pore width.

3.2. Experimental Results of NMR

According to the experimental principle of the low field NMR in Section 2.2, there is a quantitative relationship between the T_2 relaxation time of the saturated water coal sample and core pore radius r (Equation (3)). According to the experimental content, the coal structure is simplified as the columnar pipe [38], so for the parameter in Equation (3), we take F_s = 2. And then, the pore size distribution of four kinds of coal samples can be drawn, as shown in Figure 4.

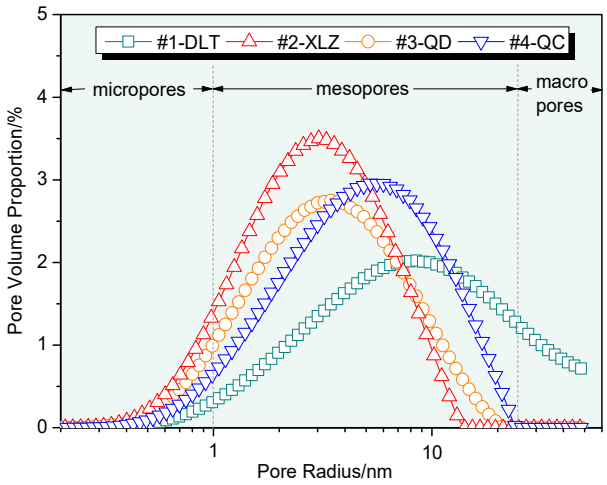

Figure 4. The pore size distributions measured by NMR.

The pore size distribution of coal sample measured by nuclear magnetic resonance is shown in Figure 4. The pore size distribution of coal sample adsorption holes in the figure is all single peak, and the maximum peak point is within the range of 2 nm–15 nm. The peak value of gas coal is the largest, followed by anthracite, coking coal, and long flame coal. Peak position from left to right is gas coal, coking coal, anthracite, long flame coal. The largest single peak area is long flame coal, followed by anthracite, gas coal, and coking coal. Due to the change of the test method, the influence mechanism of the metamorphic degree on the whole adsorption pores can be analyzed [39]. That is, for the long flame coal #1−DLT, it is in the low metamorphic stage of coal, it withstands formation pressure less, and the coal body structure is relatively loose.

4. Discussion

4.1. The Applicability of Fractal Models of the Coal Adsorption Pore Structure

Based on the theory proposed by previous scholars [40], the fractal dimension can be calculated by combining the results of the NAM with the FHH model:

$$ln(V/V_0) = C + A \times ln[ln(p_0/p) \quad (4)$$

In Equation (4), V is the volume of adsorbed N_2 at equilibrium pressure p; V_0 is the monolayer adsorption volume. p_0 is the saturated vapor pressure of adsorbed N_2; A is the slope of $ln(V/V_0)$ and $ln[ln(p_0/p)]$ in the double logarithmic coordinates; and C is the constant.

When the van der Waals force is the main adsorption force, the relationship between A and the fractal dimension D is:

$$A = \frac{D-3}{3} \quad (5)$$

When the capillary condensation occurs in pores, the surface tension is the main force, and the relationship between A and the fractal dimension D is:

$$A = D - 3 \quad (6)$$

In Equations (5) and (6), D is the fractal dimension calculated by the FHH fractal model; and A is the slope of lnV and $ln[ln(p_0/p)]$ in the double logarithmic coordinates.

The fractal dimension of adsorption pore can be calculated by this experimental method. At the same time, when using this model to calculate the fractal dimension, it is usually divided into the low-pressure section (the relative pressure is 0–0.45) and the high-pressure section (the relative pressure is 0.45–1.00) to obtain fractal dimensions of different pressure sections. The fractal dimension of the low-pressure section is set as D_1, and the fractal dimension of the high-pressure section is set as D_2. Figure 5 shows the fitting diagram of lnV and $ln[ln(p_0/p)]$ in the FHH fractal model.

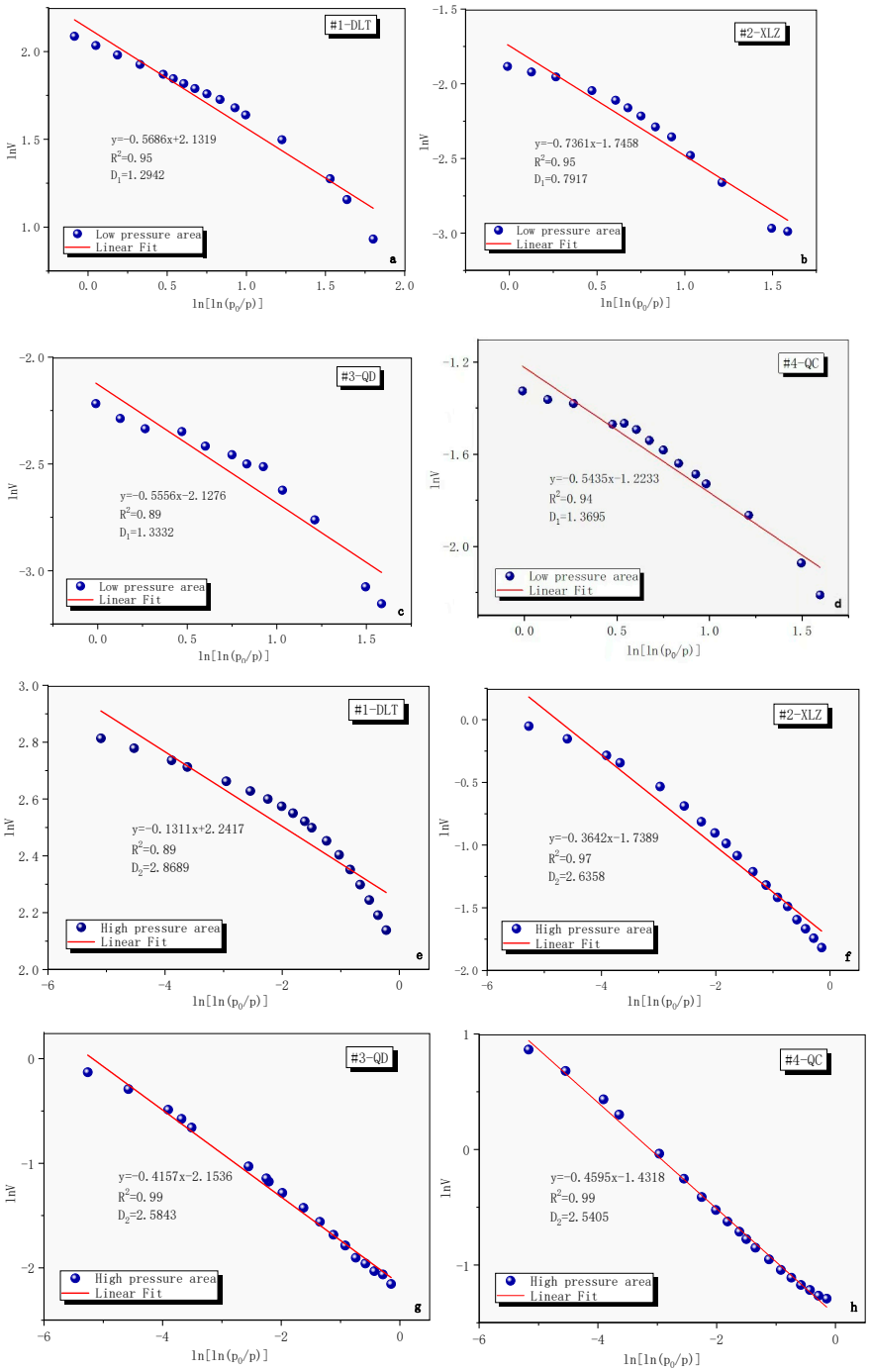

Figure 5. Fitting diagrams of $ln(V/V_0)$ and $ln[ln(p_0/p)]$.

It can be seen from Figure 6 that all fitting coefficients of four coal samples are above 0.89, that is to say, the fitting effects are good. FHH fractal model can be used to calculate the fractal dimension of adsorption pores of four coal samples, which can effectively characterize the complexity of the adsorption pore structure of coal samples. At the same time, because this model can calculate the adsorption capacity of coal, it can be used to characterize the complex pore structure of coal. This complexity represents the degree of irregularity in the coal body surface.

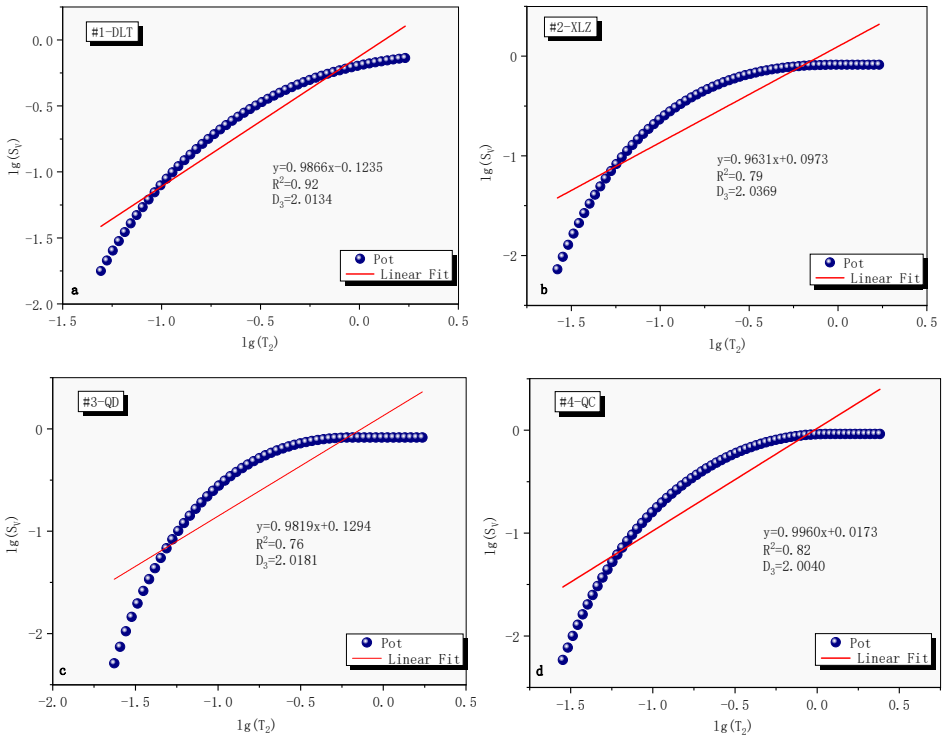

Figure 6. Fitting diagrams of $lg(T_2)$ and $lg(S_V)$.

According to an algorithm based on the capillary pressure method to calculate the fractal dimension, Zhang et al. [41] combines the T_2 spectrum distribution obtained from the NMR experiment and deduces an algorithm based on the T_2 spectrum curve to calculate the fractal dimension:

$$\lg(S_v) = (3 - D)\lg(T_2) + (D - 3)lgT_{2max} \quad (7)$$

In Equation (7), S_v is the corresponding cumulative pore volume percentage; T_2 is the transverse relaxation time; T_{2max} is the maximum transverse relaxation time; and D is the measured pore volume fractal dimension.

The fractal dimension based on the T_2 spectrum can be expressed as follows:

$$D = 3 - k \quad (8)$$

In Equation (8), k is the slope of the linear fit of $lg(T_2)$, $lg(S_V)$.

Moreover, the inflection point of the curve in the relationship curve between the logarithmic value $lg(T_2)$ of the transverse relaxation time T_2 and the logarithmic value $lg(S_V)$ of the corresponding cumulative pore volume percentage S_v in the NMR data is the boundary point between the fractal dimension of the adsorption pore volume and the fractal dimension of the seepage pore volume. The fractal dimension of adsorption pores is the volume fractal dimension, which indicates the complexity of the pore size distribution. Generally, the pore size in porous media satisfies the pore diameter $\left(\frac{\lambda_{min}}{\lambda_{max}}\right)^D \approx 0$ [42,43], so for the $\frac{\lambda_{min}}{\lambda_{max}}$ of four kinds of test samples selected 2.764 nm/95.36 nm, 1.48 nm/95.36 nm, 1.318 nm/96.46 nm,

1.134 nm/96.38 nm as the pore diameter range to calculate the fractal dimension of the overall structure of adsorption pores, and thus obtained the fractal dimension D_3. The fitting curves of $lg(T_2)$ and $lg(S_V)$ is shown in Figure 6.

Table 2 shows the calculation results of fractal dimension obtained from the above fitting curve and algorithm.

Table 2. The calculation results of fractal dimensions.

Fractal Dimensions	Test Sample			
	#1−DLT	**#2−XLZ**	**#3−QD**	**#4−QC**
D_1	1.2942	0.7917	1.3332	1.3695
D_2	2.8689	2.6358	2.5843	2.5405
D_3	2.0134	2.0369	2.0181	2.0040

From the range distribution of mesoporous fractal dimensions, there are no effective values in D_1, which are lower than 2, and all values of D_2 are between 2 and 3, indicating that D_2 is more effective. This is because in the FHH fractal model, the calculation model of the high-pressure section is based on the capillary condensation process, and the effect of surface tension is considered. For the mesopores, the capillary condensation process is a characteristic process within the pore size range, which does not occur in the micropores. Therefore, the effective fractal dimension can be obtained by using the adsorption data of the high-pressure section. However, the data of low-pressure section contain some microporous adsorption data, which affect the calculation results of fractal dimensions. Among them, D_2 mainly ranges from 2.5 to 2.9, and the value of D_2 gradually decreases with the increase of the metamorphism degree, which indicates that the complexity of mesopores decreases with the increase of the metamorphism degree [44]. The D_3 is between 2.004 and 2.0369 as the #1−DLT long flame coal has a lower D_3 fractional dimensional value due to its looser coal structure and more connected macropore network. With the exception of the #1−DLT long flame coal, the D_3 values gradually decrease with increasing metamorphism, which could indicate that the complexity of the pores throughout the adsorption pore space gradually decreases with increasing metamorphism.

The average value of D_3 is less than that of D_2, which is due to the difference between test methods and fractal models used. First, D_2 is calculated by using the FHH model and N_2 adsorption capacity, while D_3 is calculated by using the capillary beam fractal model and T_2 spectrum. Therefore, when the pore diameter is in the range of 0–100 nm, gas can enter into smaller pores more than water, which results in more complex pore structure and smaller D_3 value. Second, there are some differences in the physical meaning of characterization. The FHH model is based on the adsorption capacity to characterize the surface irregularity of coal body, while the capillary beam fractal model represents the complexity of the pore size distribution. The complexity of pore size distribution in coal is composed of micropores, mesopores, and macropores, so the D_3 change of four coal samples is not obvious. Third, except for the #1−DLT coal sample, D_2 and D_3 of the other three coal samples gradually decrease with the increase of metamorphic degree, and the variation laws are consistent, that is, the complexity of adsorption pore structure generally decreases with the increase of metamorphic degree [45].

4.2. The Relationships between Adsorption Pore Structural Parameters and Fractal Dimensions

Table 3 shows the experimental results based on the specific surface area and total pore volume of adsorption pores of coal samples obtained with NAM:

Table 3. Specific pore surface area and total pore volume of adsorption pores of 4 experimental samples.

Coal Type	Number	Specific Surface Area/($m^2 \cdot g^{-1}$)	Total Pore Volume/($cm^3 \cdot g^{-1}$)
Long flame coal	#1−DLT	10.7715	0.01712
gas coal	#2−XLZ	0.2085	0.00103
Coking coal	#3−QD	0.1354	0.00088
anthracite	#4−QC	0.2869	0.00226

From Table 3, with the increase in the metamorphism degree, the specific surface area and total pore volume of adsorption pores show the trend of first decreasing and then increasing, especially for the long flame coal. Compared with the other three coal samples, the specific surface area and total pore volume differ by 100 and 10 orders of magnitude, respectively, with significant differences. In order to further discuss the quantitative relationship between the pores and fractal dimensions of coals with different metamorphic degrees, Figure 7 shows the relationship curves between specific surface area, pore volume, and D_2 and D_3.

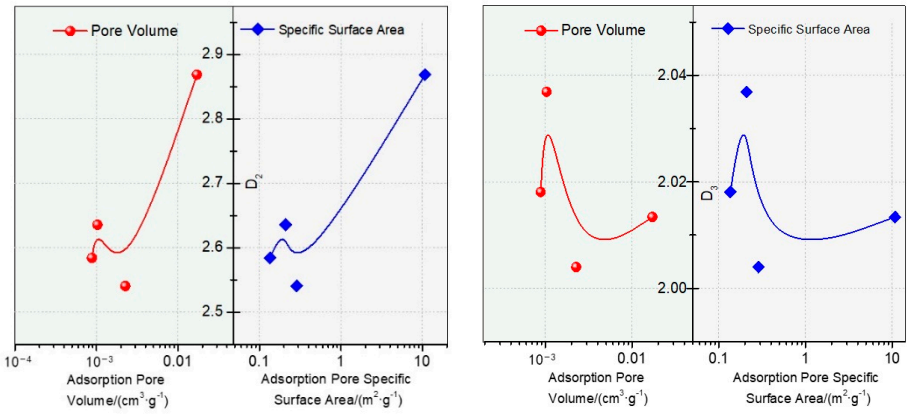

Figure 7. Relationships between structural parameters and fractal dimensions.

Figure 7 shows that the fractal dimensions of the two types first increase, then decrease, and finally increase with the increase of total pore volume and specific surface area. From these four groups of curves, it can be concluded that there are no direct quantitative relationships between the two structural parameters and the fractal dimensions D_2 and D_3, which represent the surface irregularity and the complexity of the pore size distribution, respectively [46]. In other words, the factors that determine the fractal dimension are not only determined by the pore volume or specific surface area. In order to verify this conclusion, the calculation results of the proportion of the pore volume and specific surface area of micropores, mesopores, and macropores to the whole adsorption pores are arranged in Table 4. The curves of D_2 and D_3 change with the proportion of each scale, as shown in Figure 8.

Table 4. Calculation results of the proportion of the pore volume and specific surface area of micropores, mesopores, and macropores to the whole adsorption pores.

Coal Samples	The Proportion of Pore Volume/%			The Proportion of Surface Area/%		
	Micropores	Mesopores	Macropores	Micropores	Mesopores	Macropores
#1−DLT	26.29	72.01	1.70	53.28	46.03	0.69
#2−XLZ	2.25	83.86	13.89	12.80	77.10	10.1
#3−QD	4.88	71.71	23.41	26.67	68.86	4.47
#4−QC	5.04	65.76	29.20	31.50	61.94	6.56

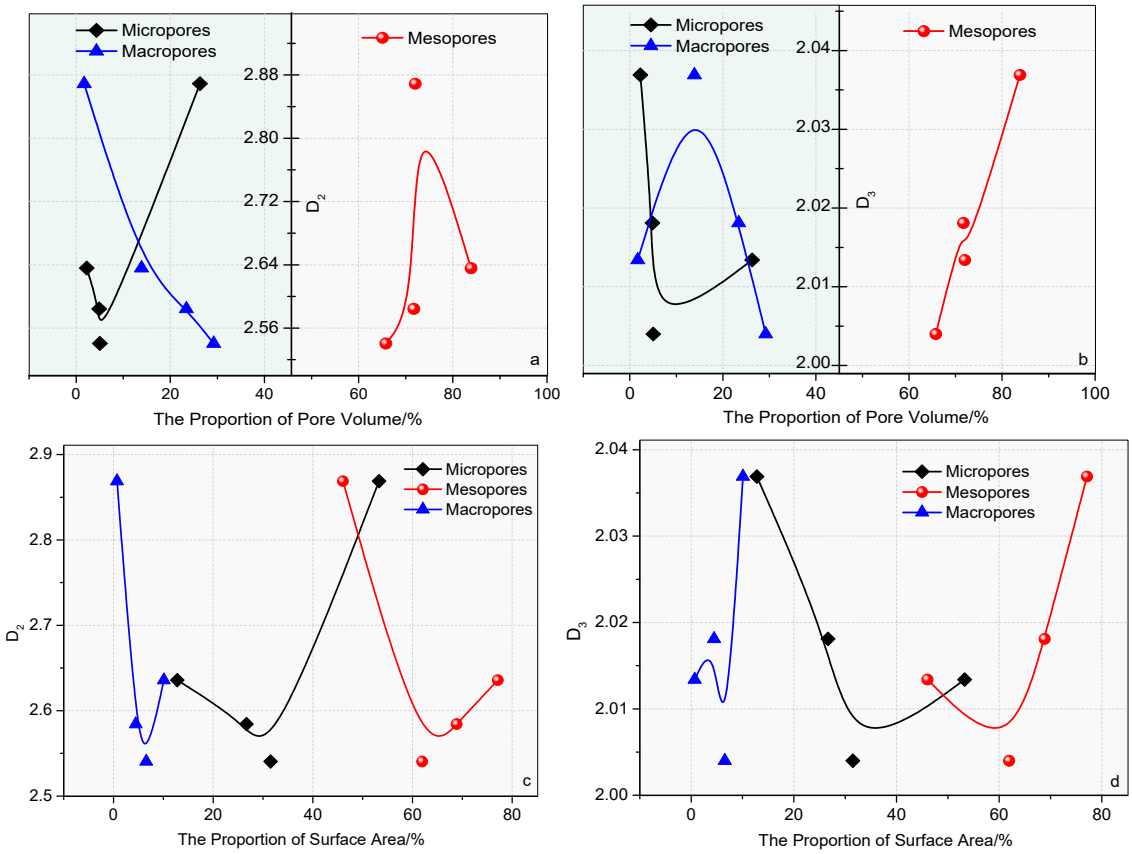

Figure 8. Relationships between proportions of pore parameters and fractal dimensions.

It can be seen from Figure 8 that there are no direct quantitative relationships between the proportions and fractal dimensions, indicating that single structural parameters do not directly determine the values of fractal dimensions [47]. Combined with Figures 3 and 4 obtained from two experiments, it can be found that for D_2, in the mesoporous scale range, the peak value of pore diameter distribution is concentrated at 2–10 nm, and the closer the highest peak point is to the range of 2–5 nm, the larger the fractal dimension value is. For D_3, in the whole adsorption pores, the single peak value of the pore diameter distribution is mainly in the range of 2–30 nm (except for the #1—DLT coal sample). Similarly, the closer the pore diameter distribution is to the range of 2–5 nm, the larger the fractal dimension value is, the higher the complexity of pore structure is.

At the same time, the influence mechanism of fractal characteristics of coal structure on its adsorption properties is discussed. Therefore, according to the results of the NAM experiment, the relationships between two fractal dimensions and the maximum nitrogen adsorption properties are drawn.

First of all, it can be seen from Figure 9a that there is a good linear positive correlation between the fractal dimension D_2 calculated by the FHH fractal model and the maximum N_2 adsorption capacity, and the correlation coefficient is 0.87, which indicates that the more complex the inner surface irregularity of coal adsorption pore structure is, the better the adsorption properties of coal is, which also indicates that the main determinant of adsorption properties of coal is the specific surface area [48–50]. Second, it can be seen from Figure 9b that there is no obvious quantitative relationship between the fractal dimension D_3 calculated by the capillary beam fractal model and the maximum N_2 adsorption capacity, which also confirms that D_3, which represents the complexity of the pore size distribution, is not the main factor affecting the adsorption performance of coal. Therefore, according to the relationships between the two fractal dimensions and the maximum adsorption properties, the physical meaning of two fractal dimensions can also be distinguished.

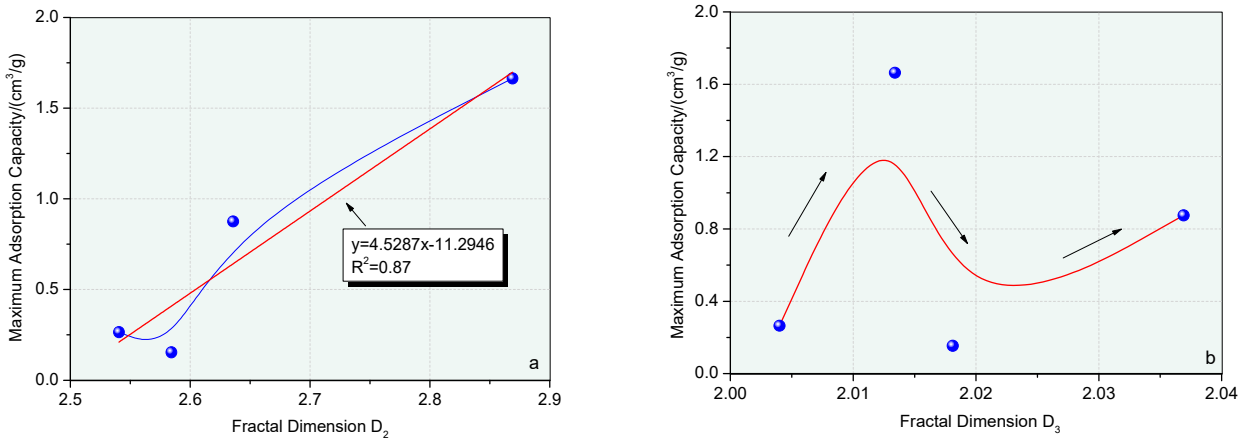

(**a**) (**b**)

Figure 9. Relationships between fractal dimensions and the maximum adsorption properties. (**a**) D_2-maximum adsorption capacity. (**b**) D_3-maximum adsorption capacity.

5. Conclusions

This paper uses the NAM and low-field NMR to conduct the multistage analyses of parameters such as the pore size distribution, pore shape, pore volume, and specific surface area of four coal samples with different metamorphism degrees. Based on the fractal models, multiple fractal dimensions are calculated. The relationships between fractal dimensions and various quantitative parameters of micropores, mesopores, macropores and whole adsorption pore structure are obtained.

(1) Combined with the metamorphism characteristics of coal, the formation pressure and temperature are constantly changing, and the rapid pyrolysis fracture of aliphatic rings in coal macromolecules results in disappearing first and then forming a large number of pores between coal molecules. Therefore, the pore volume and specific surface area of adsorption pores first decrease and then increase with the increase of the metamorphism degree.

(2) Due to the difference in fractal models, among them, the effective fractal dimensions based on the FHH fractal model are concentrated in the range of 2.5–2.9, which are suitable for the pore size range of the capillary condensation process; the effective fractal dimensions based on T_2 spectrums and the capillary bundle fractal model are concentrated in the range of 2.004–2.037.

(3) It is found that the single structure parameter of adsorption pores has no direct quantitative relationship with the fractal dimension. However, the fractal dimension has a certain relationship with the range of pore diameter distribution, that is, the more the pore size distribution is concentrated in 2–5 nm, the larger the fractal dimension value, the higher the complexity of pore structure.

(4) There is a good linear positive correlation between the fractal dimension D_2 which characterizes the degree of surface irregularity in the coal body and the maximum nitrogen adsorption capacity, with a correlation coefficient of 0.87, indicating that the greater the degree of surface irregularity in the coal body, the better the coal body's adsorption performance.

Author Contributions: Writing—original draft preparation, W.W.; methodology, data curation, writing, Z.L.; methodology, data processing, validation, English polish, M.Z.; methodology, data processing, H.Y. All authors have read and agreed to the published version of the manuscript.

Funding: The authors would like to acknowledge the support of the National Natural Science Foundation of China (52274213, 52074173, 51934004), Natural Science Foundation of Shandong Province (ZR2022YQ52), and Taishan Scholars Project Special Funding (TS20190935).

Data Availability Statement: Not applicable.

Acknowledgments: The authors would like to acknowledge the support of the National Natural Science Foundation of China (52074173, 51604168, 51934004), the Key Research and Development Plan of Shandong Province, China (2019GSF111033), Major Program of Shandong Province Natural Science Foundation (ZR2018ZA0602) and Taishan Scholars Project Special Funding (TS20190935).

Conflicts of Interest: All authors declare that there is no conflict of interest.

References

1. Feng, R.; Liu, J.; Harpalani, S. Optimized pressure pulse-decay method for laboratory estimation of gas permeability of sorptive reservoirs: Part 1—Background and numerical analysis. *Fuel* **2017**, *191*, 555–564. [CrossRef]
2. Xia, L.; Yin, Y.; Yu, X.; Zheng, Y. An approach to grading coalbed methane resources in China for the purpose of implementing a differential production subsidy. *Pet. Sci.* **2019**, *16*, 447–457. [CrossRef]
3. Sulaiman, W.R.W.; Azizan, N.; Jaafar, M.Z.; Ismail, A.R.; Hamid, M.A.; Johari, A.; Mat, R.; Kamaruddin, M.J.; Ali, A. Additional gas resource for coal bed methane by applying underground coal gasification and enhanced coal bed methane. In Proceedings of the 5th KKU International Engineering Conference 2014, KKU-IENC 2014, Khon Kaen, Thailand, 27–29 March 2014; Trans Tech Publications Ltd.: Khon Kaen, Thailand, 2014.
4. Du, F.; Wang, K. Unstable failure of gas-bearing coal-rock combination bodies: Insights from physical experiments and numerical simulations. *Process. Saf. Environ. Prot.* **2019**, *129*, 264–279. [CrossRef]
5. Wang, K.; Du, F. Coal-gas compound dynamic disasters in China: A review. *Process. Saf. Environ. Prot.* **2019**, *133*, 1–17. [CrossRef]
6. Wang, K.; Guo, Y.; Wang, G.; Du, F. Seepage and Mechanical Failure Characteristics of Gas-bearing Composite Coal-Rock under True Triaxial Path. *J. China Coal Soc.* **2023**, *10*, 13225.
7. Kim, Y.-M.; Jang, H.-C.; Lee, J.-H. Application of probabilistic approach to evaluate coalbed methane resources using geological data of coal basin in Indonesia. *Geosci. J.* **2015**, *20*, 229–238. [CrossRef]
8. Wang, Z.; Cheng, Y.; Qi, Y.; Wang, R.; Wang, L.; Jiang, J. Experimental study of pore structure and fractal characteristics of pulverized intact coal and tectonic coal by low temperature nitrogen adsorption. *Powder Technol.* **2019**, *350*, 15–25. [CrossRef]
9. Feng, R.; Chen, S.; Bryant, S.; Liu, J. Stress-dependent permeability measurement techniques for unconventional gas reservoirs: Review, evaluation, and application. *Fuel* **2019**, *256*, 115987. [CrossRef]
10. Sang, S.X.; Zhu, Y.M.; Zhang, S.; Zhang, J.; Tang, J.X. Solid-gas action mechanism of coal adsorption gas(I)—Coal pore structure and solid gas action. *Nat. Gas Ind.* **2005**, *25*, 13–15+205. (In Chinese)
11. Zhang, Y.H.; Lebedev, M.; Al-Yaseri, A.; Yu, H.Y.; Xu, X.M.; Iglauer, S. Characterization of nanoscale rock mechanical properties and microstructures of a Chinese sub-bituminous coal. *J. Nat. Gas Sci. Eng.* **2018**, *52*, 106–116. [CrossRef]
12. Yang, H.; Cheng, W.; Liu, Z.; Wang, W.; Zhao, D.; Yang, W. Study on the dynamic evolution law of the effective stress in the coal seam water infusion process based on fractal theory. *Fractals* **2020**, *28*, 73–76. [CrossRef]
13. Liu, Z.; Wang, W.; Yang, H.; Yu, S.; Xin, L. Experimental Study on the Fractal Pattern of a Coal Body Pore Structure Around a Water Injection Bore. *J. Energy Resour. Technol.* **2020**, *142*, 012302. [CrossRef]
14. Feng, Z.; Zhou, D.; Zhao, Y.; Cai, T. Study on microstructural changes of coal after methane adsorption. *J. Nat. Gas Sci. Eng.* **2016**, *30*, 28–37. [CrossRef]
15. Meng, M.; Qiu, Z. Experiment study of mechanical properties and microstructures of bituminous coals influenced by supercritical carbon dioxide. *Fuel* **2018**, *219*, 223–238. [CrossRef]
16. Zhang, W.J.; Ju, Y.W.; Wei, M.M.; Wang, G.C. Study on characteristics and mechanism of adsorption/desorption on different metamorphic-deformed coal reservoirs. *Earth Sci. Front.* **2015**, *22*, 232–242.
17. Chen, M.-Y.; Cheng, Y.-P.; Li, H.-R.; Wang, L.; Jin, K.; Dong, J. Impact of inherent moisture on the methane adsorption characteristics of coals with various degrees of metamorphism. *J. Nat. Gas Sci. Eng.* **2018**, *55*, 312–320. [CrossRef]
18. Niu, Q.; Pan, J.; Jin, Y.; Wang, H.; Li, M.; Ji, Z.; Wang, K.; Wang, Z. Fractal study of adsorption-pores in pulverized coals with various metamorphism degrees using N2 adsorption, X-ray scattering and image analysis methods. *J. Pet. Sci. Eng.* **2019**, *176*, 584–593. [CrossRef]
19. Li, P.; Zhang, X.; Zhang, S. Structures and fractal characteristics of pores in low volatile bituminous deformed coals by low-temperature N_2 adsorption after different solvents treatments. *Fuel* **2018**, *224*, 661–675. [CrossRef]
20. Zhang, J.; Wei, C.; Yan, G.; Lu, G. Structural and fractal characterization of adsorption pores of middle–high rank coal reservoirs in western Yunnan and eastern Guizhou: An experimental study of coals from the Panguan syncline and Laochang anticline. *Energy Explor. Exploit.* **2018**, *37*, 251–272. [CrossRef]
21. Liu, Z.; Wang, W.; Cheng, W.; Yang, H.; Zhao, D. Study on the seepage characteristics of coal based on the Kozeny-Carman equation and nuclear magnetic resonance experiment. *Fuel* **2020**, *266*, 117088. [CrossRef]
22. Deng, G.-Z.; Zheng, R. Micropore Structure and Fractal Characteristics of Low-Permeability Coal Seams. *Adv. Mater. Sci. Eng.* **2018**, *2018*, 4186280. [CrossRef]
23. Zhang, B.; Liu, W.; Liu, X. Scale-dependent nature of the surface fractal dimension for bi- and multi-disperse porous solids by mercury porosimetry. *Appl. Surf. Sci.* **2006**, *253*, 1349–1355. [CrossRef]
24. Liu, X.; Nie, B. Fractal characteristics of coal samples utilizing image analysis and gas adsorption. *Fuel* **2016**, *182*, 314–322. [CrossRef]

25. Yao, Y.; Liu, D.; Tang, D.; Tang, S.; Huang, W. Fractal characterization of adsorption-pores of coals from North China: An investigation on CH4 adsorption capacity of coals. *Int. J. Coal Geol.* **2008**, *73*, 27–42. [CrossRef]
26. Cai, Y.; Liu, D.; Yao, Y.; Li, J.; Liu, J. Fractal characteristics of coal pores based on classic geometry and thermodynamics models. *Acta Geol. Sin. Engl. Ed.* **2011**, *85*, 1150–1162. [CrossRef]
27. Lu, G.; Wang, J.; Wei, C.; Song, Y.; Yan, G.; Zhang, J.; Chen, G. Pore fractal model applicability and fractal characteristics of seepage and adsorption pores in middle rank tectonic deformed coals from the Huaibei coal field. *J. Pet. Sci. Eng.* **2018**, *171*, 808–817. [CrossRef]
28. Song, H.; Min, L.; Jun, X.; Lushi, S.; Peisheng, L.; Sheng, S.; Xuexin, S. Fractal characteristic of three Chinese coals. *Fuel* **2004**, *83*, 1307–1313. [CrossRef]
29. Liu, Z.; Yang, H.; Wang, W.; Cheng, W.; Xin, L. Experimental Study on the Pore Structure Fractals and Seepage Characteristics of a Coal Sample Around a Borehole in Coal Seam Water Infusion. *Transp. Porous Media* **2018**, *125*, 289–309. [CrossRef]
30. Hu, L.; Zhu, Y.M.; Chen, S.B.; Du, Z.L. Fractal characteristics of pore structure of Longmaxi formation shale in Shuanghe, southern Sichuan. *Xinjiang Pet. Geol.* **2013**, *34*, 79–82. (In Chinese)
31. Zhou, S.; Liu, D.; Cai, Y.; Yao, Y. Fractal characterization of pore–fracture in low-rank coals using a low-field NMR relaxation method. *Fuel* **2016**, *181*, 218–226. [CrossRef]
32. Wang, G.; Han, D.; Qin, X.; Liu, Z.; Liu, J. A comprehensive method for studying pore structure and seepage characteristics of coal mass based on 3D CT reconstruction and NMR. *Fuel* **2020**, *281*, 118735. [CrossRef]
33. Yi, M.; Cheng, Y.; Wang, Z.; Wang, C.; Hu, B.; He, X. Effect of particle size and adsorption equilibrium time on pore structure characterization in low pressure N2 adsorption of coal: An experimental study. *Adv. Powder Technol.* **2020**, *31*, 4275–4281. [CrossRef]
34. Rouquerol, J.; Avnir, D.; Fairbridge, C.W.; Everett, D.H.; Haynes, J.M.; Pernicone, N.; Ramsay, J.D.F.; Sing, K.S.W.; Unger, K.K. Recommendations for the characterization of porous soilds. *Pure Appl. Chem.* **1994**, *66*, 1739–1758. [CrossRef]
35. Luo, L.; Yao, W.; Liu, J.; Zhang, H.; Ma, J.; Jiang, X. Evolution of NOX precursors of superfine pulverized coal with a fixed bed in N_2 and CO_2. *Fuel* **2018**, *234*, 263–275. [CrossRef]
36. Dai, F.Y.; Hu, H.Y.; Zhang, A.H. Suitability study on fractal model of organic shale pore. *Coal Sci. Technol.* **2019**, *47*, 168–175.
37. Sing, K.S.W.; Everett, D.H.; Haul, R.A.W. Reporting physisorption data for gas solid systems with special reference to the determination of surface area and porosity. *Pure Appl. Chem.* **1985**, *57*, 603–619. [CrossRef]
38. Xiao, L.Z. *NMR Imaging Logging Principles and Applications*; Science Press: Beijing, China, 1998.
39. Li, J.Q.; Yao, Y.B.; Cai, Y.D. Discussion on coal physical properties and formation with different metamorphic degree in north China. *Coal Sci. Technol.* **2012**, *40*, 111–115.
40. Davies, S.; Packer, K.J. Pore size distributions from nuclear magnetic resonance spin-lattice relaxation measurements of fluid-saturated porous solids. *Theory Simul. J. Appl. Phys.* **1990**, *67*, 3163–3170. [CrossRef]
41. Zhang, Y.T.; Wang, D.M.; Zhong, X.X. Features of fissure sharp in coal borehole and variation law with temperature. *Coal Sci. Technol.* **2007**, *35*, 73–76. (In Chinese)
42. Yu, B.M.; Xu, P.; Zou, M.Q.; Cai, J.C.; Zheng, Q. *Fractal Porous Media Transport Physics*; Science Press: Beijing, China, 2014.
43. Chen, J.; Cheng, W.; Wang, G.; Li, H. Effect of dominated coal pores and fractures on water migration after low-pressure water injection based on CT images. *Fuel* **2021**, *307*, 121795. [CrossRef]
44. Wang, K.; Guo, Y.; Du, F.; Dong, H.; Xu, C. Effect of the water injection pressure on coal permeability based on the pore-fracture fractal characteristics: An experimental study. *Greenh. Gases Sci. Technol.* **2021**, *12*, 136–147. [CrossRef]
45. Sun, B.; Yang, Q.; Zhu, J.; Shao, T.S.; Yang, Y.H.; Hou, C.Y.; Li, G.Y. Pore size distributions and pore multifractal characteristics of medium and low-rank coals. *Nat. Res.* **2020**, *10*, 22353. [CrossRef] [PubMed]
46. Zeng, Q.; Luo, M.; Pang, X.; Li, L.; Li, K. Surface fractal dimension: An indicator to characterize the microstructure of cement-based porous materials. *Appl. Surf. Sci.* **2013**, *282*, 302–307. [CrossRef]
47. Xia, Y.; Cai, J.; Perfect, E.; Wei, W.; Zhang, Q.; Meng, Q. Fractal dimension, lacunarity and succolarity analyses on CT images of reservoir rocks for permeability prediction. *J. Hydrol.* **2019**, *579*, 124198. [CrossRef]
48. Xu, S.; Hu, E.; Li, X.; Xu, Y. Quantitative Analysis of Pore Structure and Its Impact on Methane Adsorption Capacity of Coal. *Nat. Resour. Res.* **2021**, *30*, 605–620. [CrossRef]
49. Karolina, W.R.; Natalia, H.; Adam, S. Effect of porous structure of coal on propylene adsorption from gas mixtures. *Sci. Rep.* **2020**, *10*, 11277.
50. Artioli, Y. Adsorption. *Encycl. Ecol.* **2008**, *4*, 60–65.